Higher-Order DGFEM Transport Calculations on Polytope Meshes for Massively-Parallel Architectures

Michael W. Hackemack

Chair: Jean C. Ragusa
Committee Members: Marvin L. Adams, Jim E. Morel, Nancy M. Amato
External Advisor: Troy Becker

Department of Nuclear Engineering
Texas A&M University
College Station, TX, USA 77843

mike_hack@tamu.edu

Outline

1. Overview
   - The DGFEM S_N Transport Equation
   - Motivation for this Work
2. Polytope Finite Element Basis Functions
   - Linear Basis Functions on 2D Polygons
   - Quadratic Serendipity Basis Functions on 2D Polygons
   - Linear Basis Functions on 3D Polyhedra
3. Diffusion Synthetic Acceleration on Polytopes
   - Theory
   - MIP Diffusion Form
4. Proposed Work and Current Status
5. Work Summary

The Continuous-Energy Transport Equation

Transport Equation

$$\left[\mathbf{\Omega} \cdot \nabla + \sigma_t(\mathbf{r}, E)\right] \psi(\mathbf{r}, E, \mathbf{\Omega}) = \int_{4\pi} \int_0^\infty \sigma_s(\mathbf{r}, E', E, \mathbf{\Omega}', \mathbf{\Omega}) \psi(\mathbf{r}, E', \mathbf{\Omega}') dE' d\Omega' + Q(\mathbf{r}, E, \mathbf{\Omega})$$

Boundary Conditions

$$\psi(\mathbf{r}, E, \mathbf{\Omega}) = \psi^{inc}(\mathbf{r}, E, \mathbf{\Omega}) + \int_{\mathbf{\Omega}' \cdot \mathbf{n} < 0} \int_0^\infty \beta(\mathbf{r}, E', E, \mathbf{\Omega}', \mathbf{\Omega}) \psi(\mathbf{r}, E', \mathbf{\Omega}') dE' d\Omega'$$

Term Definitions

$\mathbf{r}$ - neutron position
E - neutron energy
$\mathbf{\Omega}$ - neutron solid angle
$\psi(\mathbf{r}, E, \mathbf{\Omega})$ - angular flux
$Q(\mathbf{r}, E, \mathbf{\Omega})$ - distributed neutron source
$\sigma_t(\mathbf{r}, E)$ - total macroscopic cross section
$\sigma_s(\mathbf{r}, E', E, \mathbf{\Omega}', \mathbf{\Omega})$ - total macroscopic scattering cross section
$\beta(\mathbf{r}, E', E, \mathbf{\Omega}', \mathbf{\Omega})$ - boundary albedo

Energy and Angular Discretization

The multigroup S_N equations

$$(\mathbf{\Omega}_m \cdot \nabla + \sigma_{t,g})\,\psi_{m,g} = \sum_{g'=1}^{G} \sum_{k=0}^{N_k} \frac{2p+1}{4\pi} \sigma_{s,k}^{g' \to g} \sum_{n=-k}^{k} \phi_{k,n,g'} Y_{k,n}(\mathbf{\Omega}_m) + Q_{m,g}$$

Multigroup Method

$$\psi_g = \int_{\Delta E_g} \psi(E)\,dE, \qquad \Delta E_g \in [E_g, E_{g-1}]$$

$$\sigma_{t,g} = \frac{\int_{\Delta E_g} \sigma_t(E)\,\psi(E)\,dE}{\int_{\Delta E_g} \psi(E)\,dE}$$

Spherical Harmonics

$$\phi_{k,n} \equiv \int_{4\pi} d\Omega\,\psi(\mathbf{\Omega})\,Y_{k,n}(\mathbf{\Omega}),$$

$$\sigma_{s,k} \equiv \int_{-1}^{1} d\mu\,\sigma_s(\mu_0) P_k(\mu_0)$$

$$\mu_0 \equiv \mathbf{\Omega}' \cdot \mathbf{\Omega}$$

$$\sigma_s(\mathbf{\Omega}' \cdot \mathbf{\Omega}) \equiv \frac{1}{2\pi} \sigma_s(\mu_0)$$

$$P_k(\mathbf{\Omega}' \cdot \mathbf{\Omega}) \equiv \frac{1}{2\pi} P_k(\mu_0)$$

Spatial Discretization - 1 group/direction and general source

Multiply element K by basis functions and apply Gauss theorem

$$-\left(\boldsymbol{\Omega}_m \cdot \nabla b_m, \psi_m\right)_K + \sum_{f=1}^{N_f^K} \left\langle \left(\boldsymbol{\Omega}_m \cdot \mathbf{n}_f\right) b_m, \tilde{\psi}_m \right\rangle_f + \left(\sigma_t b_m, \psi_m\right)_K = \left(b_m, Q_m\right)_K$$

The upwind scheme

$$\tilde{\psi}_m(\mathbf{r}) = \begin{cases} \psi_m^-, & \partial K^+ \\ \psi_m^+, & \partial K^- \backslash \partial \mathcal{D} \\ \psi_m^{inc}, & \partial K^- \cap \partial \mathcal{D}^d \\ \psi_{m'}^-, & \partial K^- \cap \partial \mathcal{D}^r \end{cases} \qquad \psi_m^{\pm}(\mathbf{r}) \equiv \lim_{s \to 0^{\pm}} \psi_m\Big(\mathbf{r} + s(\boldsymbol{\Omega}_m \cdot \mathbf{n})\mathbf{n}\Big)$$

Full set of equations for element K

$$\begin{aligned} -\Big(\boldsymbol{\Omega}_m \cdot \nabla b_m, \psi_m\Big)_K + \Big(\sigma_t b_m, \psi_m\Big)_K + \left\langle \left(\boldsymbol{\Omega}_m \cdot \mathbf{n}\right) b_m, \psi_m^- \right\rangle_{\partial K^+} \\ + \left\langle \left(\boldsymbol{\Omega}_m \cdot \mathbf{n}\right) b_m, \psi_m^+ \right\rangle_{\partial K^- \backslash \partial \mathcal{D}} + \left\langle \left(\boldsymbol{\Omega}_m \cdot \mathbf{n}\right) b_m, \psi_{m'}^- \right\rangle_{\partial K^- \cap \partial \mathcal{D}^r} \\ = \left(b_m, Q_m\right)_K + \left\langle \left(\boldsymbol{\Omega}_m \cdot \mathbf{n}\right) b_m, \psi_m^{inc} \right\rangle_{\partial K^- \cap \partial \mathcal{D}^d} \end{aligned}$$

Spatial Discretization - 1 group/direction and general source

Multiply element K by basis functions and apply Gauss theorem

$$-\left(\mathbf{\Omega}_m \cdot \nabla b_m, \psi_m\right)_K + \sum_{f=1}^{N_f^K} \left\langle \left(\mathbf{\Omega}_m \cdot \mathbf{n}_f\right) b_m, \tilde{\psi}_m \right\rangle_f + \left(\sigma_t b_m, \psi_m\right)_K = \left(b_m, Q_m\right)_K$$

The upwind scheme

$$\tilde{\psi}_m(\mathbf{r}) = \begin{cases} \psi_m^-, & \partial K^+ \\ \psi_m^+, & \partial K^- \setminus \partial \mathcal{D} \\ \psi_m^{inc}, & \partial K^- \cap \partial \mathcal{D}^d \\ \psi_{m'}^-, & \partial K^- \cap \partial \mathcal{D}^r \end{cases} \qquad \psi_m^{\pm}(\mathbf{r}) \equiv \lim_{s \to 0^{\pm}} \psi_m\Big(\mathbf{r} + s(\mathbf{\Omega}_m \cdot \mathbf{n})\mathbf{n}\Big)$$

Full set of equations for element K

$$-\left(\mathbf{\Omega}_m \cdot \nabla b_m, \psi_m\right)_K + \left(\sigma_t b_m, \psi_m\right)_K + \left\langle \left(\mathbf{\Omega}_m \cdot \mathbf{n}\right) b_m, \psi_m^- \right\rangle_{\partial K^+}$$
$$+ \left\langle \left(\mathbf{\Omega}_m \cdot \mathbf{n}\right) b_m, \psi_m^+ \right\rangle_{\partial K^- \setminus \partial \mathcal{D}} + \left\langle \left(\mathbf{\Omega}_m \cdot \mathbf{n}\right) b_m, \psi_{m'}^- \right\rangle_{\partial K^- \cap \partial \mathcal{D}^r}$$
$$= \left(b_m, Q_m\right)_K + \left\langle \left(\mathbf{\Omega}_m \cdot \mathbf{n}\right) b_m, \psi_m^{inc} \right\rangle_{\partial K^- \cap \partial \mathcal{D}^d}$$

Spatial Discretization - 1 group/direction and general source

Multiply element K by basis functions and apply Gauss theorem

$$-\left(\boldsymbol{\Omega}_m \cdot \nabla b_m, \psi_m\right)_K + \sum_{f=1}^{N_f^K} \left\langle \left(\boldsymbol{\Omega}_m \cdot \mathbf{n}_f\right) b_m, \tilde{\psi}_m \right\rangle_f + \left(\sigma_t b_m, \psi_m\right)_K = \left(b_m, Q_m\right)_K$$

The upwind scheme

$$\tilde{\psi}_m(\mathbf{r}) = \begin{cases} \psi_m^-, & \partial K^+ \\ \psi_m^+, & \partial K^- \backslash \partial \mathcal{D} \\ \psi_m^{inc}, & \partial K^- \cap \partial \mathcal{D}^d \\ \psi_{m'}^-, & \partial K^- \cap \partial \mathcal{D}^r \end{cases} \qquad \psi_m^{\pm}(\mathbf{r}) \equiv \lim_{s \to 0^{\pm}} \psi_m\Big(\mathbf{r} + s(\boldsymbol{\Omega}_m \cdot \mathbf{n})\mathbf{n}\Big)$$

Full set of equations for element K

$$\begin{aligned} -\Big(\boldsymbol{\Omega}_m \cdot \nabla b_m, \psi_m\Big)_K + \Big(\sigma_t b_m, \psi_m\Big)_K + \Big\langle \left(\boldsymbol{\Omega}_m \cdot \mathbf{n}\right) b_m, \psi_m^- \Big\rangle_{\partial K^+} \\ + \Big\langle \left(\boldsymbol{\Omega}_m \cdot \mathbf{n}\right) b_m, \psi_m^+ \Big\rangle_{\partial K^- \backslash \partial \mathcal{D}} + \Big\langle \left(\boldsymbol{\Omega}_m \cdot \mathbf{n}\right) b_m, \psi_{m'}^- \Big\rangle_{\partial K^- \cap \partial \mathcal{D}^r} \\ = \left(b_m, Q_m\right)_K + \Big\langle \left(\boldsymbol{\Omega}_m \cdot \mathbf{n}\right) b_m, \psi_m^{inc} \Big\rangle_{\partial K^- \cap \partial \mathcal{D}^d} \end{aligned}$$

Iterative Procedure

Classic Source Iteration

$$\psi^{(\ell+1)} = \mathbf{L}^{-1}\left(\mathbf{M}\boldsymbol{\Sigma}\phi^{(\ell)} + \mathbf{Q}\right)$$
$$\phi^{(\ell+1)} = \mathbf{D}\psi^{(\ell+1)}$$

Operator Terms

L - streaming + collision operator
M - moment-to-discrete operator
D - discrete-to-moment operator
Σ - scattering operator
Q - source operator

Transport Sweep

The operation $\mathbf{L}^{-1}$ can be performed in different ways. For this work, we will use the matrix-free, full-domain transport sweep.

Optically thick problems can cause slow convergence rates

Source Iteration Approximate Spectral Radius

$$\rho^{(k+1)} \approx \frac{||\phi^{(k+1)} - \phi^{(k)}||}{||\phi^{(k)} - \phi^{(k-1)}||}$$

Optically Thick Cases - leakage/absorption does not dominate

- $\sigma_s^{g\to g}/\sigma_{t,g} \approx 1$ and $(\sigma_{t,g} \cdot \text{diam}(\mathcal{D})) \gg 1$
- Thermal upscattering into higher energy groups is significant

Answer - Precondition the transport sweep

- Diffusion Synthetic Acceleration (DSA)
- Transport Synthetic Acceleration (TSA)
- Boundary Projection Acceleration (BPA)
- etc.

Optically thick problems can cause slow convergence rates

Source Iteration Approximate Spectral Radius

$$\rho^{(k+1)} \approx \frac{||\phi^{(k+1)} - \phi^{(k)}||}{||\phi^{(k)} - \phi^{(k-1)}||}$$

Optically Thick Cases - leakage/absorption does not dominate

- $\sigma_s^{g\to g}/\sigma_{t,g} \approx 1$ and $(\sigma_{t,g} \cdot \text{diam}(\mathcal{D})) \gg 1$
- Thermal upscattering into higher energy groups is significant

Answer - Precondition the transport sweep

- Diffusion Synthetic Acceleration (DSA)
- Transport Synthetic Acceleration (TSA)
- Boundary Projection Acceleration (BPA)
- etc.

Higher-Order FEM Motivation

FEM convergence rate - no solution irregularity

$$||u - u_h||_{L_2} = C\, h^{p+1}, \qquad ||u - u_h||_{L_2} = C\, N_{dof}^{-\frac{p+1}{d}}$$

C - error constant dependent on mesh, basis function, and polynomial order
h - maximum diameter for an element
p - polynomial order of the finite element basis
N_{dof} - total degrees of freedom: $N_{dof} \propto h^{-d}$
d - dimensionality of the problem (*i.e.,* 1,2,3)

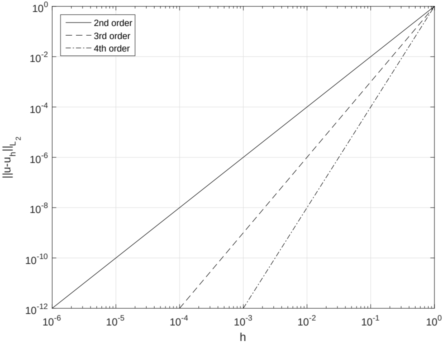

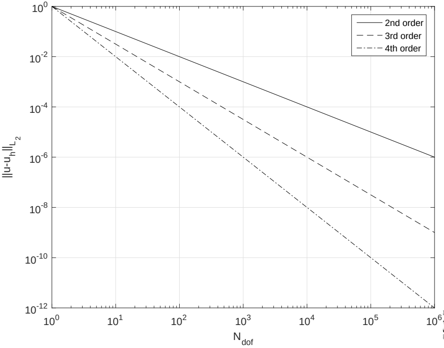

Polytope Grid Motivation

- Other physics communities are now employing polytope grids due to decreased cell/face counts (CFD in particular)
- They allow for transition elements between different domain regions
- Hanging nodes from non-conforming meshes are not necessary
- Independently-generated simplicial grids (*i.e.* created in parallel) can be stitched together with polytopes without communicating the whole mesh across processors

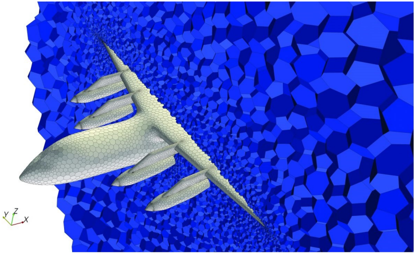

Polytope Grid Motivation

- Other physics communities are now employing polytope grids due to decreased cell/face counts (CFD in particular)
- They allow for transition elements between different domain regions
- Hanging nodes from non-conforming meshes are not necessary
- Independently-generated simplicial grids (*i.e.* created in parallel) can be stitched together with polytopes without communicating the whole mesh across processors

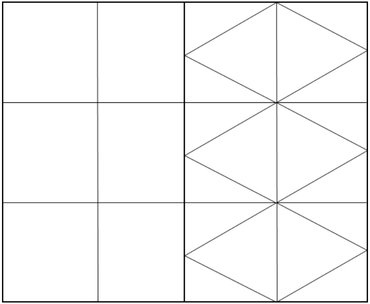

Polytope Grid Motivation

- Other physics communities are now employing polytope grids due to decreased cell/face counts (CFD in particular)
- They allow for transition elements between different domain regions
- Hanging nodes from non-conforming meshes are not necessary
- Independently-generated simplicial grids (*i.e.* created in parallel) can be stitched together with polytopes without communicating the whole mesh across processors

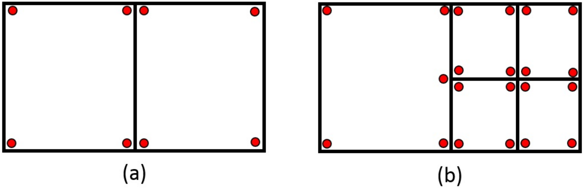

Polytope Grid Motivation

- Other physics communities are now employing polytope grids due to decreased cell/face counts (CFD in particular)
- They allow for transition elements between different domain regions
- Hanging nodes from non-conforming meshes are not necessary
- Independently-generated simplicial grids (*i.e.* created in parallel) can be stitched together with polytopes without communicating the whole mesh across processors

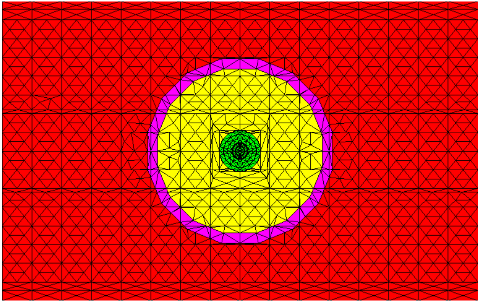

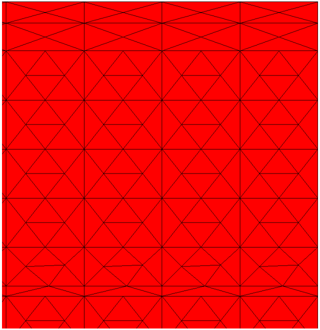

Polytope Finite Elements

2D arbitrary convex/concave polygons

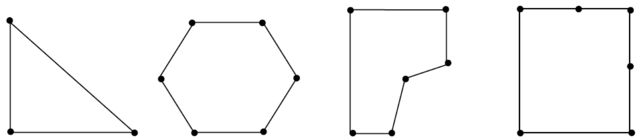

3D convex polyhedra

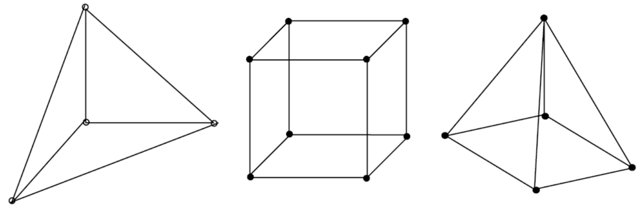

A common class of linear finite elements - the $\mathbb{P}_1$ space

2D $\mathbb{P}_1$ space - reference element

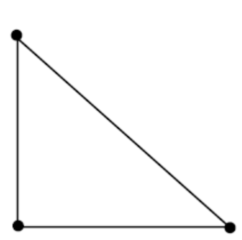

$$\lambda_1(r,s) = 1 - r - s$$
$$\lambda_2(r,s) = r$$
$$\lambda_3(r,s) = s$$

3D $\mathbb{P}_1$ space - reference element

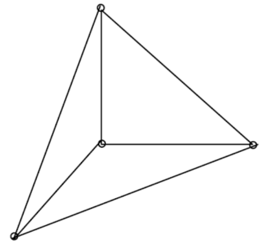

$$\lambda_1(r,s,t) = 1 - r - s - t$$
$$\lambda_2(r,s,t) = r$$
$$\lambda_3(r,s,t) = s$$
$$\lambda_4(r,s,t) = t$$

Linear Basis Functions on 2D Polygons

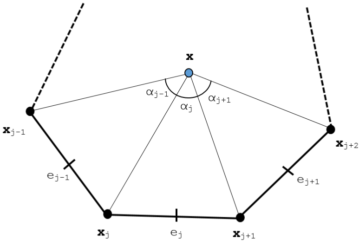

Basis Function Properties - Barycentric Coordinates

λ_i - linear basis function located at vertex i

1. $\lambda_i \geq 0$
2. $\sum_i \lambda_i = 1$
3. $\sum_i \mathbf{x}_i \lambda_i(\mathbf{x}) = \mathbf{x}$
4. $\lambda_i(\mathbf{x}_j) = \delta_{ij}$

Linear Basis Functions on 2D Polygons

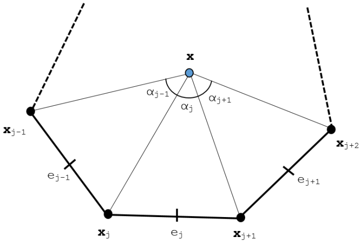

Linear basis functions that we consider

1. Wachspress rational coordinates*
2. Piecewise linear (PWL) coordinates*
3. Mean value coordinates
4. Maximum entropy coordinates

*have been previously analyzed for transport problems

Wachspress Rational Functions (Go to extra)

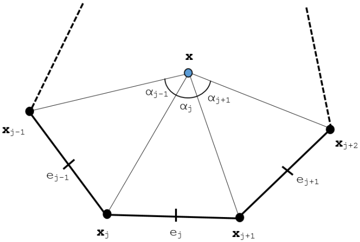

$$\lambda_i^W(\mathbf{x}) = \frac{w_i(\mathbf{x})}{\sum_j w_j(\mathbf{x})}, \qquad w_j(\mathbf{x}) = \frac{A(\mathbf{x}_{j-1}, \mathbf{x}_j, \mathbf{x}_{j+1})}{A(\mathbf{x}, \mathbf{x}_{j-1}, \mathbf{x}_j)\, A(\mathbf{x}, \mathbf{x}_j, \mathbf{x}_{j+1})}$$

$$A(\mathbf{x}_1, \mathbf{x}_2, \mathbf{x}_3) = \frac{1}{2} \begin{vmatrix} 1 & 1 & 1 \\ x_1 & x_2 & x_3 \\ y_1 & y_2 & y_3 \end{vmatrix}$$

TEXAS A&M ENGINEERING

Piecewise Linear (PWL) Functions

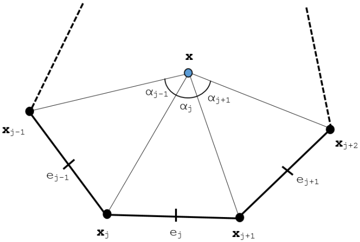

$$\lambda_i^{PWL}(\mathbf{x}) = t_i(\mathbf{x}) + \alpha_i t_c(\mathbf{x})$$

t_i - standard 2D linear function for a triangle $(i, i+1, C)$; 1 at vertex i that linearly decreases to 0 to the cell center and the adjoining vertices

t_c - 2D tent function; 1 at cell center and linearly decreases to 0 to each cell vertex

$\alpha_i = \frac{1}{N_V}$ - weight parameter for vertex i

N_V - number of cell vertices

Mean Value Coordinates (Go to extra)

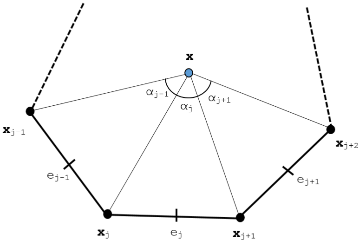

Preserve piecewise linear harmonic maps over triangulations

$$\frac{\partial^2 u}{\partial x^2} + \frac{\partial^2 u}{\partial y^2} = 0, \qquad u(\mathbf{r}) = u_0,\ \mathbf{r} \in \partial\mathcal{D}$$

$u(\mathbf{r})$ - piecewise linear function on the cell boundary

Mean Value Coordinates (Go to extra)

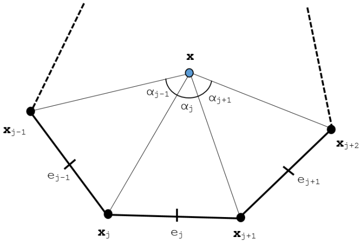

$$\lambda_i^{MV}(\mathbf{x}) = \frac{w_i(\mathbf{x})}{\sum_j w_j(\mathbf{x})}, \qquad w_j(\mathbf{x}) = \frac{\tan(\alpha_{j-1}/2) + \tan(\alpha_j/2)}{|\mathbf{x}_j - \mathbf{x}|}$$

Limit as $\mathbf{x} \to \mathbf{x}_j$

$$\lim_{\mathbf{x}\to\mathbf{x}_j} \tan(\alpha_{j-1}/2) + \tan(\alpha_j/2) = 0 \qquad \longrightarrow \qquad \lim_{\mathbf{x}\to\mathbf{x}_j} w_j(\mathbf{x}) = 1$$

Maximum Entropy Coordinates (Go to extra)

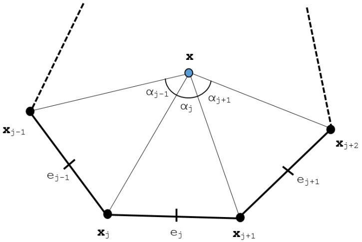

Constrained optimization problem - Shannon Entropy

$$\max_{\lambda(\mathbf{x})} H(\lambda, m), \qquad H(\lambda, m) = -\sum_i \lambda_i(\mathbf{x}) \ln\left(\frac{\lambda_i(\mathbf{x})}{m_i(\mathbf{x})}\right)$$

$$\sum_i \lambda_i(\mathbf{x}) = 1, \qquad \sum_i \lambda_i(\mathbf{x})(\mathbf{x}_i - \mathbf{x}) = \mathbf{0}$$

Maximum Entropy Coordinates (Go to extra)

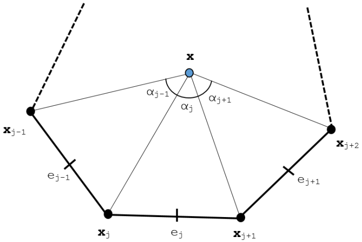

$$\lambda_i^{ME}(\mathbf{x}) = \frac{w_i(\mathbf{x})}{\sum_j w_j(\mathbf{x})}, \qquad w_j(\mathbf{x}) = m_j(\mathbf{x}) \exp(-\omega^* \cdot (\mathbf{x}_j - \mathbf{x}))$$

$$\mathcal{L}(\lambda, \omega_0, \omega) = -\sum_i \lambda_i(\mathbf{x}) \ln\left(\frac{\lambda_i(\mathbf{x})}{m_i(\mathbf{x})}\right) - \omega_0 \left(\sum_i \lambda_i(\mathbf{x}) - 1\right) - \omega \cdot \left(\sum_i \lambda_i(\mathbf{x})(\mathbf{x}_i - \mathbf{x})\right)$$

Maximum Entropy Coordinates (Go to extra)

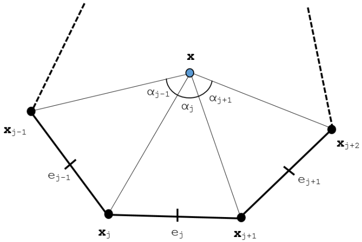

$$\lambda_i^{ME}(\mathbf{x}) = \frac{w_i(\mathbf{x})}{\sum_j w_j(\mathbf{x})}, \qquad w_j(\mathbf{x}) = m_j(\mathbf{x}) \exp(-\omega^* \cdot (\mathbf{x}_j - \mathbf{x}))$$

$$\omega^* = \operatorname{argmin} F(\omega, \mathbf{x}) \qquad F(\omega, \mathbf{x}) = \ln\left(\sum_j w_j(\mathbf{x})\right)$$

Finite element architecture

Mass Matrix - element K

$$\mathbf{M}^K = \int_K d\mathbf{r}\, \lambda(\mathbf{x})\, \lambda^T(\mathbf{x}) = \sum_{q=1}^{N_q^K} w_q^K\, \lambda(\mathbf{x}_q^K)\, \lambda^T(\mathbf{x}_q^K)$$

Advection Matrix - element K

$$\mathbf{G}^K = \int_K d\mathbf{r}\, \nabla\lambda(\mathbf{x})\, \lambda^T(\mathbf{x}) = \sum_{q=1}^{N_q^K} w_q^K\, \nabla\lambda(\mathbf{x}_q^K)\, \lambda^T(\mathbf{x}_q^K)$$

Surface Matrix - face f for element K

$$\mathbf{N}_f^K = \int_f ds\, \lambda(\mathbf{x})\, \lambda^T(\mathbf{x}) = \sum_{q=1}^{N_f} w_q^f\, \lambda(\mathbf{x}_q^f)\, \lambda^T(\mathbf{x}_q^f)$$

Summary of the 2D Linear Basis Functions

Basis Function	Dimension	Polytope Types	Integration	Direct/Iterative
Wachspress	2D/3D	Convex*	Numerical	Direct
PWL	1D/2D/3D	Convex/Concave	Analytical	Direct
Mean Value	2D**	Convex/Concave	Numerical	Direct
Max Entropy	1D/2D/3D	Convex/Concave	Numerical	Iterative***

* - weak convexity for Wachspress coordinates does not cause blow up
** - mean value 3D analogue only applicable triangular-faceted polyhedra
*** - maximum entropy minimization solved via Newton's Method

Quadratic Serendipity Basis Functions on 2D Polygons

1. Form the linear barycentric functions - $\{\lambda_i\}$
2. Construct the pairwise products - $\{\mu_{ab}\}$
3. Eliminate the interior nodes to form a serendipity basis - $\{\xi_{ij}\}$

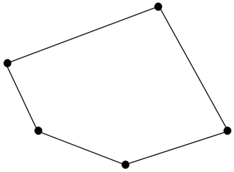

$\{\lambda_i\}$
Linear

Quadratic Serendipity Basis Functions on 2D Polygons

1. Form the linear barycentric functions - $\{\lambda_i\}$
2. Construct the pairwise products - $\{\mu_{ab}\}$
3. Eliminate the interior nodes to form a serendipity basis - $\{\xi_{ij}\}$

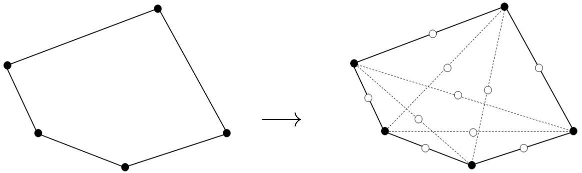

$\{\lambda_i\}$
Linear

$\{\mu_{ab}\}$
Quadratic

Quadratic Serendipity Basis Functions on 2D Polygons

1. Form the linear barycentric functions - $\{\lambda_i\}$
2. Construct the pairwise products - $\{\mu_{ab}\}$
3. Eliminate the interior nodes to form a serendipity basis - $\{\xi_{ij}\}$

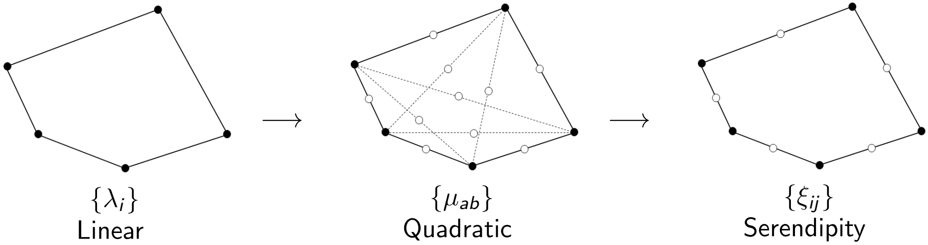

Pairwise products of the barycentric basis functions - $\mu_{ab} = \lambda_a \lambda_b$

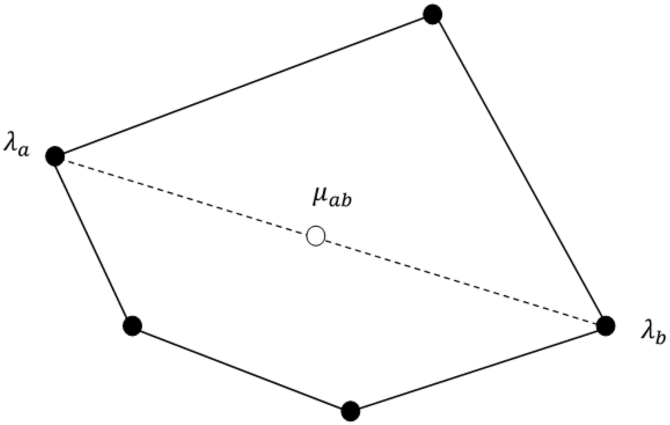

TEXAS A&M ENGINEERING

Pairwise products of the barycentric basis functions - $\mu_{ab} = \lambda_a \lambda_b$

Necessary Precision Properties

$$\sum_{aa \in V} \mu_{aa} + \sum_{ab \in E \cup D} 2\mu_{ab} = 1$$

$$\sum_{aa \in V} \mathbf{x}_{aa}\mu_{aa} + \sum_{ab \in E \cup D} 2\mathbf{x}_{ab}\mu_{ab} = \mathbf{x}$$

$$\sum_{aa \in V} \mathbf{x}_a \mathbf{x}_a^T \mu_{aa} + \sum_{ab \in E \cup D} \left(\mathbf{x}_a \mathbf{x}_b^T + \mathbf{x}_b \mathbf{x}_a^T \right) \mu_{ab} = \mathbf{x}\mathbf{x}^T$$

V - vertex nodes
E - face midpoint nodes
D - interior diagonal nodes

$$V + E + D = n + n + \frac{n(n-3)}{2}$$

Further Notation/Notes

$$\mathbf{x}_{ab} = \frac{\mathbf{x}_a + \mathbf{x}_b}{2}, \qquad \mu_{ab} = \lambda_a \lambda_b$$

$$\mu_{ab}^K(\mathbf{r}) = 0, \qquad \{ab \in D, \mathbf{r} \in \partial K\}$$

Eliminate interior nodes to form serendipity basis

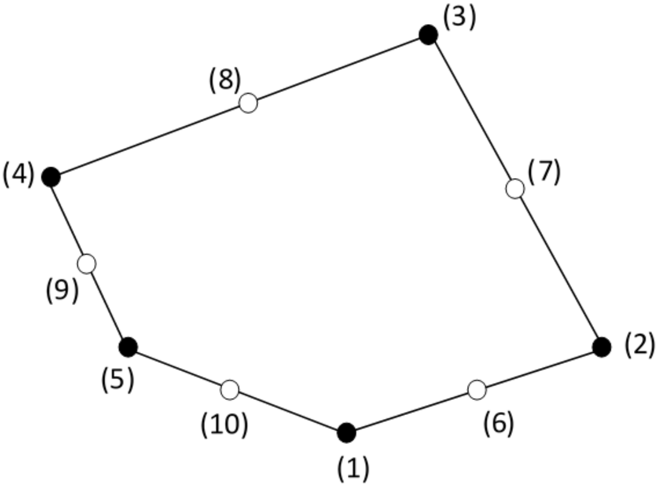

Eliminate interior nodes to form serendipity basis

Serendipity Precision Properties

$$\sum_{ii \in V} \xi_{ii} + \sum_{i(i+1) \in E} 2\xi_{i(i+1)} = 1$$

$$\sum_{ii \in V} \mathbf{x}_{ii}\xi_{ii} + \sum_{i(i+1) \in E} 2\mathbf{x}_{i(i+1)}\xi_{i(i+1)} = \mathbf{x}$$

$$\sum_{ii \in V} \mathbf{x}_i \mathbf{x}_i^T \xi_{ii} + \sum_{i(i+1) \in E} \left(\mathbf{x}_i \mathbf{x}_{i+1}^T + \mathbf{x}_{i+1} \mathbf{x}_i^T \right) \xi_{i(i+1)} = \mathbf{x}\mathbf{x}^T$$

ξ_{ii} - basis function at vertex i

$\xi_{i(i+1)}$ - basis function at face midpoint between vertices $(i, i+1)$

Reduction Problem - $[\xi] := \mathbb{A}\,[\mu]$

$$\mathbb{A} = \begin{bmatrix} c_{11}^{11} & \dots & c_{ab}^{11} & \dots & c_{(n-2)n}^{11} \\ \dots & \ddots & \vdots & \ddots & \vdots \\ c_{11}^{ij} & \dots & c_{ab}^{ij} & \dots & c_{(n-2)n}^{ij} \\ \dots & \ddots & \vdots & \ddots & \vdots \\ c_{11}^{n(n+1)} & \dots & c_{ab}^{n(n+1)} & \dots & c_{(n-2)n}^{n(n+1)} \end{bmatrix}$$

Eliminate interior nodes to form serendipity basis

Constant Precision

$$\sum_{ii \in V} c_{aa}^{ii} + \sum_{i(i+1) \in E} 2c_{aa}^{i(i+1)} = 1, \qquad \forall aa \in V$$

$$\sum_{ii \in V} c_{ab}^{ii} + \sum_{i(i+1) \in E} 2c_{ab}^{i(i+1)} = 2, \qquad \forall ab \in E \cup D$$

Linear Precision

$$\sum_{ii \in V} c_{aa}^{ii} \mathbf{x}_{ii} + \sum_{i(i+1) \in E} 2c_{aa}^{i(i+1)} \mathbf{x}_{i(i+1)} = \mathbf{x}_{aa}, \qquad \forall aa \in V$$

$$\sum_{ii \in V} c_{ab}^{ii} \mathbf{x}_{ii} + \sum_{i(i+1) \in E} 2c_{ab}^{i(i+1)} \mathbf{x}_{i(i+1)} = 2\mathbf{x}_{ab}, \qquad \forall ab \in E \cup D$$

Quadratic Precision

$$\sum_{ii \in V} c_{aa}^{ii} \mathbf{x}_i \mathbf{x}_i^T + \sum_{i(i+1) \in E} c_{aa}^{i(i+1)} \left(\mathbf{x}_i \mathbf{x}_{i+1}^T + \mathbf{x}_{i+1} \mathbf{x}_i^T \right) = \mathbf{x}_a \mathbf{x}_a^T, \qquad \forall aa \in V$$

$$\sum_{ii \in V} c_{ab}^{ii} \mathbf{x}_i \mathbf{x}_i^T + \sum_{i(i+1) \in E} c_{ab}^{i(i+1)} \left(\mathbf{x}_i \mathbf{x}_{i+1}^T + \mathbf{x}_{i+1} \mathbf{x}_i^T \right) = \mathbf{x}_a \mathbf{x}_b^T + \mathbf{x}_b \mathbf{x}_a^T, \qquad \forall ab \in E \cup D$$

Special case - bilinear coordinates on the unit square

Bilinear coordinates and quadratic extension

$$
\begin{aligned}
\lambda_1 &= (1-x)(1-y) \\
\lambda_2 &= x(1-y) \\
\lambda_3 &= xy \\
\lambda_4 &= (1-x)y
\end{aligned}
$$

$$
\begin{aligned}
\mu_{11} &= (1-x)^2(1-y)^2 & \mu_{12} &= (1-x)x(1-y)^2 \\
\mu_{22} &= x^2(1-y)^2 & \mu_{23} &= x^2y(1-y) \\
\mu_{33} &= x^2y^2 & \mu_{34} &= (1-x)xy^2 \\
\mu_{44} &= (1-x)^2y^2 & \mu_{41} &= (1-x)^2y(1-y) \\
\mu_{13} &= (1-x)x(1-y)y & \mu_{24} &= (1-x)x(1-y)y
\end{aligned}
$$

Reduction matrix

$$
\mathbb{A} = \begin{bmatrix}
1 & 0 & 0 & 0 & 0 & 0 & 0 & 0 & -1 & 0 \\
0 & 1 & 0 & 0 & 0 & 0 & 0 & 0 & 0 & -1 \\
0 & 0 & 1 & 0 & 0 & 0 & 0 & 0 & -1 & 0 \\
0 & 0 & 0 & 1 & 0 & 0 & 0 & 0 & 0 & -1 \\
0 & 0 & 0 & 0 & 1 & 0 & 0 & 0 & 1/2 & 1/2 \\
0 & 0 & 0 & 0 & 0 & 1 & 0 & 0 & 1/2 & 1/2 \\
0 & 0 & 0 & 0 & 0 & 0 & 1 & 0 & 1/2 & 1/2 \\
0 & 0 & 0 & 0 & 0 & 0 & 0 & 1 & 1/2 & 1/2
\end{bmatrix}
$$

Serendipity coordinates

$$
\begin{aligned}
\xi_{11} &= (1-x)(1-y)(1-x-y) \\
\xi_{22} &= x(1-y)(x-y) \\
\xi_{33} &= xy(-1+x+y) \\
\xi_{44} &= (1-x)y(y-x) \\
\xi_{12} &= (1-x)x(1-y) \\
\xi_{23} &= xy(1-y) \\
\xi_{34} &= (1-x)xy \\
\xi_{41} &= (1-x)y(1-y)
\end{aligned}
$$

Linear Basis Functions on 3D Polyhedra

Linear basis functions and convex polyhedra only for 3D

- The 2D quadratic serendipity formulation is more arduous in 3D
- Intercell coupling is not straightforward for concave polyhedra
- Focus on 3D PWL functions
- Focus on 3D parallelepipeds and extruded convex polygons (convex prisms)

3D PWL basis functions

$$b_i(\mathbf{x}) = t_i(\mathbf{x}) + \sum_{f=1}^{F_i} \beta_f^i t_f(\mathbf{x}) + \alpha_i t_c(\mathbf{x})$$

t_i - standard 3D linear function for a tet $(i, i+1, f_c, K_c)$; 1 at vertex i, linearly decreases to 0 to the cell center, each adjoining face center, and each adjoining vertex

t_c - 3D tent function; 1 at cell center, linearly decreases to 0 at all vertices and face centers

t_f - face tent function; 1 at face center, linearly decreases to 0 at each face vertex and cell center

$\alpha_i = \frac{1}{N_V}$ - weight parameter for vertex i

$\beta_f^i = \frac{1}{N_f}$ - weight parameter for face f touching vertex i

Diffusion Synthetic Acceleration

Transport iteration and error

$$\mathbf{L}\psi = \mathbf{B}\phi + \mathbf{C}\phi + \mathbf{Q}$$

$$\mathbf{L}\psi^{(\ell+1/2)} = \mathbf{B}\phi^{(\ell+1/2)} + \mathbf{C}\phi^{(\ell)} + \mathbf{Q}$$

$$\mathbf{L}\delta\psi^{(\ell+1/2)} - \mathbf{B}'\delta\phi^{(\ell+1/2)} = \mathbf{R}^{(\ell+1/2)}$$

$$\delta\psi^{(\ell+1/2)} \equiv \psi - \psi^{(\ell+1/2)}$$

$$\delta\phi^{(\ell+1/2)} \equiv \mathbf{D}\delta\psi^{(\ell+1/2)}$$

Error approximation and update

If we could exactly solve for the error, then the solution could be obtained immediately:

$$\phi^{(\ell+1)} = \phi^{(\ell+1/2)} + \delta\phi^{(\ell+1/2)}$$

However, this is just as difficult as the full transport problem. Instead, we estimate the error using low-order operators:

$$\tilde{\mathbf{L}}\delta\psi^{(\ell+1/2)} - \tilde{\mathbf{B}}'\delta\phi^{(\ell+1/2)} = \tilde{\mathbf{R}}^{(\ell+1/2)}$$

Various DSA Implementations

Historical DSA Work

- Kopp & Lebedev - independently proposed method
- Gelbard and Hageman (G&B) - efficient convergence on fine meshes
- Reed - showed that G&B diverged for coarse meshes
- Alcouffe - consistency yields efficiency and robustness

Fully-consistent DSA schemes

- Larsen fully-consistent four step
- Fully-consistent DSA (FCDSA)

Partially-consistent DSA schemes

- Modified four step (M4S)
- Waering-Larsen-Adams (WLA)
- Modified Interior Penalty DSA (MIP)

Various DSA Implementations

Historical DSA Work

- Kopp & Lebedev - independently proposed method
- Gelbard and Hageman (G&B) - efficient convergence on fine meshes
- Reed - showed that G&B diverged for coarse meshes
- Alcouffe - consistency yields efficiency and robustness

Fully-consistent DSA schemes

- Larsen fully-consistent four step
- Fully-consistent DSA (FCDSA)

Partially-consistent DSA schemes

- Modified four step (M4S)
- Waering-Larsen-Adams (WLA)
- Modified Interior Penalty DSA (MIP)

The diffusion equation is used as our low-order operator

The Diffusion Equation

$$-\nabla \cdot D\nabla\Phi(\mathbf{r}) + \sigma\Phi(\mathbf{r}) = q(\mathbf{r}), \qquad \mathbf{r} \in \mathcal{D}$$

General Boundary Conditions

$$\begin{aligned} \Phi(\mathbf{r}) &= \Phi_0(\mathbf{r}), & \mathbf{r} \in \partial\mathcal{D}^d \\ -D\partial_n\Phi(\mathbf{r}) &= J_0(\mathbf{r}), & \mathbf{r} \in \partial\mathcal{D}^n \\ \frac{1}{4}\Phi(\mathbf{r}) + \frac{1}{2}D\partial_n\Phi(\mathbf{r}) &= J^{inc}(\mathbf{r}), & \mathbf{r} \in \partial\mathcal{D}^r \end{aligned}$$

Desirable diffusion form properties

- Discontinuous form
- Agnostic of directionality of interior faces
- Can handle concave and degenerate polytope cells
- Symmetric Positive-Definite (SPD)
- Availability of suitable preconditioners

Symmetric Interior Penalty (SIP) Form

Bilinear Form

$$
\begin{aligned}
a(\Phi, b) = \Big\langle D\nabla\Phi, \nabla b \Big\rangle_{\mathcal{D}} + \Big\langle \sigma\Phi, b \Big\rangle_{\mathcal{D}} \\
+\Big\{ \kappa_e^{SIP} [\![\Phi]\!], [\![b]\!] \Big\}_{E_h^i} - \Big\{ [\![\Phi]\!], \{\{ D\partial_n b \}\} \Big\}_{E_h^i} - \Big\{ \{\{ D\partial_n \Phi \}\}, [\![b]\!] \Big\}_{E_h^i} \\
+\Big\{ \kappa_e^{SIP} \Phi, b \Big\}_{\partial\mathcal{D}^d} - \Big\{ \Phi, D\partial_n b \Big\}_{\partial\mathcal{D}^d} - \Big\{ D\partial_n \Phi, b \Big\}_{\partial\mathcal{D}^d} + \frac{1}{2}\Big\{ \Phi, b \Big\}_{\partial\mathcal{D}^r}
\end{aligned}
$$

Linear Form

$$
\begin{aligned}
\ell(b) = \Big\langle q, b \Big\rangle_{\mathcal{D}} - \Big\{ J_0, b \Big\}_{\partial\mathcal{D}^n} + 2\Big\{ J_{inc}, b \Big\}_{\partial\mathcal{D}^r} \\
+\Big\{ \kappa_e^{SIP} \Phi_0, b \Big\}_{\partial\mathcal{D}^d} - \Big\{ \Phi_0, D\partial_n b \Big\}_{\partial\mathcal{D}^d}
\end{aligned}
$$

TEXAS A&M ENGINEERING

SIP Penalty Coefficient

$$\kappa_e^{SIP} \equiv \begin{cases} \frac{C_B}{2}\left(\frac{D^+}{h^+} + \frac{D^-}{h^-}\right) & , e \in E_h^i \\ C_B \frac{D^-}{h^-} & , e \in \partial \mathcal{D} \end{cases}$$

$$C_B = cp(p+1)$$

c - user defined constant ($c \geq 1$)
p - polynomial order of the finite element basis $(1, 2, 3, ...)$
$D^{(+/-)}$ - diffusion coefficient defined on the positive/negative side of a face
$h^{(+/-)}$ - orthogonal projection defined on the positive/negative side of a face

$$u^{\pm} = \lim_{s \to 0^{\pm}} u(\mathbf{r} + s\mathbf{n})$$

Modified Interior Penalty (MIP) Form

Diffusion Form

$$
\begin{aligned}
&\left\langle D\nabla\delta\Phi, \nabla b\right\rangle_{\mathcal{D}} + \left\langle \sigma\delta\Phi, b\right\rangle_{\mathcal{D}} \\
&+\left\{\kappa_e^{MIP}[\![\delta\Phi]\!], [\![b]\!]\right\}_{E_h^i} - \left\{[\![\delta\Phi]\!], \{\{D\partial_n b\}\}\right\}_{E_h^i} - \left\{\{\{D\partial_n\delta\Phi\}\}, [\![b]\!]\right\}_{E_h^i} \\
&+\left\{\kappa_e^{MIP}\delta\Phi, b\right\}_{\partial\mathcal{D}^{vac}} - \frac{1}{2}\left\{\delta\Phi, D\partial_n b\right\}_{\partial\mathcal{D}^{vac}} - \frac{1}{2}\left\{D\partial_n\delta\Phi, b\right\}_{\partial\mathcal{D}^{vac}} \\
&= \left\langle R, b\right\rangle_{\mathcal{D}} + \left\{\delta J_{inc}, b\right\}_{\partial\mathcal{D}^{ref}}
\end{aligned}
$$

MIP Penalty Term

$$
\kappa_e^{MIP} = \max\left(\frac{1}{4}, \kappa_e^{SIP}\right)
$$

Two-Grid Acceleration - Ideal for graphite and heavy-water configurations

Multigroup system of equations

$$\mathbf{L}\psi_g = \mathbf{M}\sum_{g'=0}^{G}\mathbf{S}_{gg'}\phi_{g'} + \mathbf{Q}_g$$

$$\mathbf{L}\psi_g^{(k+1/2)} = \mathbf{M}\sum_{g'=0}^{g}\mathbf{S}_{gg'}\phi_{g'}^{(k+1/2)} + \mathbf{M}\sum_{g'=g+1}^{G}\mathbf{S}_{gg'}\phi_{g'}^{(k)} + \mathbf{Q}_g$$

Error and residual

$$\mathbf{L}\delta\Psi_g^{(k+1/2)} = \mathbf{M}\sum_{g'=0}^{g}\mathbf{S}_{gg'}\delta\Phi_{g'}^{(k+1/2)} + \mathbf{R}_g^{(k+1/2)}$$

$$\mathbf{R}_g^{(k+1/2)} = \mathbf{M}\sum_{g'=g+1}^{G}\mathbf{S}_{gg'}\left(\Phi_{g'}^{(k+1/2)} - \Phi_{g'}^{(k)}\right)$$

Solution update

$$\delta\Phi_g^{(k+1/2)} = \epsilon^{(k+1/2)}\xi_g, \qquad \sum_{g=0}^{G}\xi_g = 1$$

1G Error Diffusion System

$$\nabla\cdot\left\langle D\right\rangle\nabla\epsilon + \left\langle\sigma\right\rangle\epsilon = \left\langle R\right\rangle$$

$$\left\langle D\right\rangle = \sum_{g=0}^{G} D_g\xi_g$$

$$\left\langle\sigma\right\rangle = \sum_{g=0}^{G}\left(\sigma_{t,g}\xi_g - \sum_{g'=0}^{G}\sigma_{s,0}^{gg'}\xi_g\right)$$

$$\left\langle R\right\rangle = \sum_{g=0}^{G} R_g^{(k+1/2)}$$

Two-Grid Acceleration - Ideal for graphite and heavy-water configurations

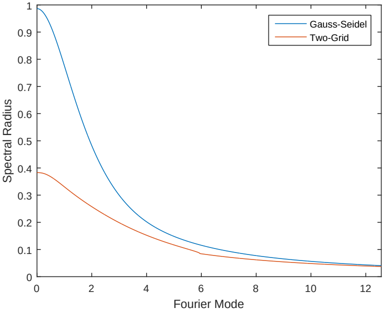

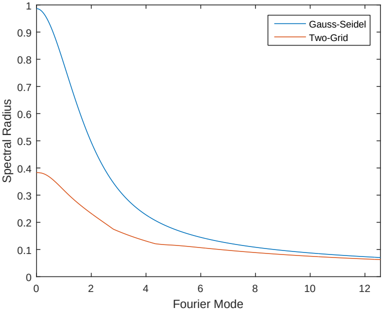

Proposed Work

POLYFEM

1. Analyze the 2D linear polygonal basis functions for use in DGFEM transport calculations
2. Perform the same analysis with the quadratic serendipity basis functions
3. Determine the effects of numerical integration on highly-distorted polygonal elements
4. Perform analysis on benchmark cases using polygonal meshes (including AMR)

MIP DSA

1. Analyze the 2D polygonal basis functions with MIP DSA preconditioning through Fourier/numerical analysis
2. Analyze the effects of AMR with polygonal basis functions on the MIP DSA PCG iteration counts (with and without bootstrapping)
3. Extend the analysis of MIP DSA to arbitrary convex 3D polyhedra
4. Implement MIP DSA in PDT using HYPRE
    1. Analyze the scalability of the method to high process counts
    2. Implement and perform analysis of two-grid acceleration
    3. Perform parametric studies on aggregation/partitioning factors - generate a performance model of MIP DSA with HYPRE
    4. Run realistic numerical experiments - IM1 and reactor geometries

2D Exactly-Linear Transport Solutions - mean value coordinates

$$\mu \frac{\partial \psi}{\partial x} + \eta \frac{\partial \psi}{\partial y} + \sigma_t \psi = Q(x, y, \mu, \eta)$$

$$\psi(x, y, \mu, \eta) = ax + by + c\mu + d\eta + e, \qquad \phi(x, y) = 2\pi\left(ax + by + e\right)$$

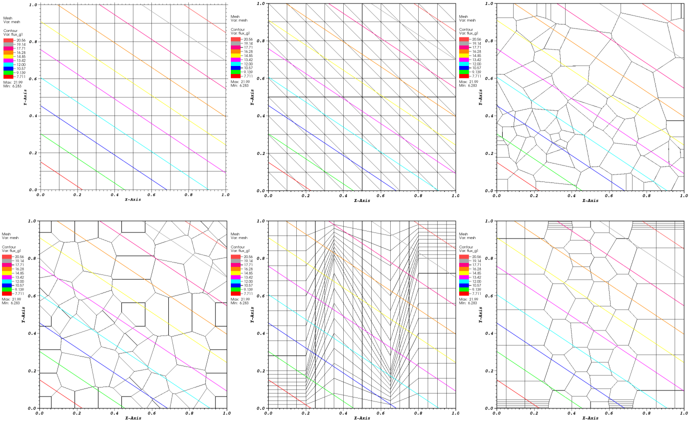

Convergence rates using MMS for the 2D polygonal basis functions

$$\psi(x,y) = \sin(\nu \frac{\pi x}{L_x}) \sin(\nu \frac{\pi y}{L_y})$$

$$\phi(x,y) = 2\pi \sin(\nu \frac{\pi x}{L_x}) \sin(\nu \frac{\pi y}{L_y})$$

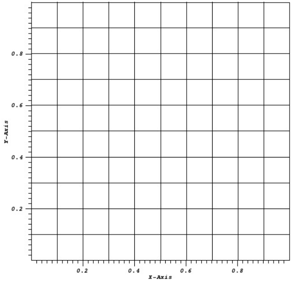

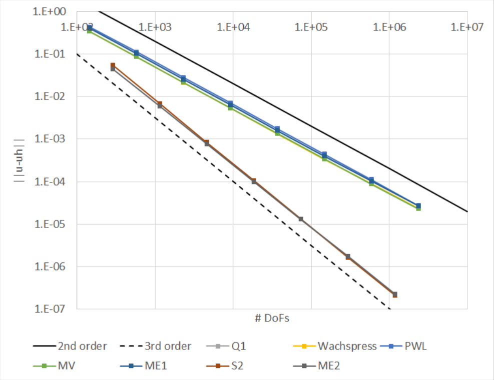

Convergence rates using MMS for the 2D polygonal basis functions

$$\psi(x,y) = \sin(\nu\frac{\pi x}{L_x})\sin(\nu\frac{\pi y}{L_y})$$

$$\phi(x,y) = 2\pi\sin(\nu\frac{\pi x}{L_x})\sin(\nu\frac{\pi y}{L_y})$$

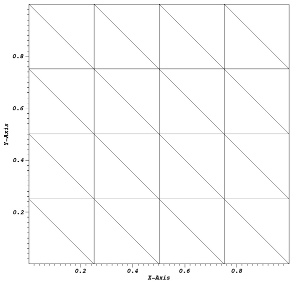

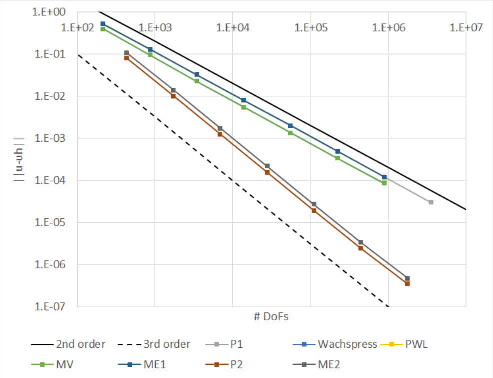

Convergence rates using MMS for the 2D polygonal basis functions

$$\psi(x,y) = \sin(\nu \frac{\pi x}{L_x}) \sin(\nu \frac{\pi y}{L_y})$$

$$\phi(x,y) = 2\pi \sin(\nu \frac{\pi x}{L_x}) \sin(\nu \frac{\pi y}{L_y})$$

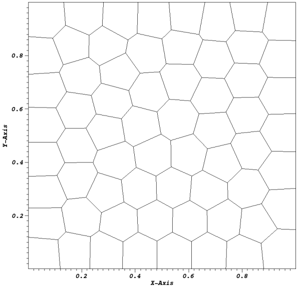

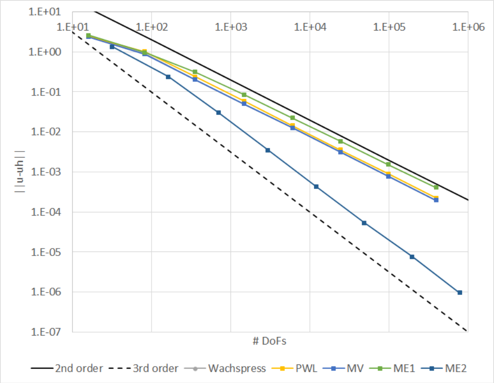

TEXAS A&M ENGINEERING

Convergence rates using MMS and AMR for the 2D polygonal basis functions

$$\psi(x,y) = x(L_x - x)y(L_y - y)\exp\left(-\frac{(x-x_0)^2 + (y-y_0)^2}{\gamma}\right),$$

$$\phi(x,y) = 2\pi x(L_x - x)y(L_y - y)\exp\left(-\frac{(x-x_0)^2 + (y-y_0)^2}{\gamma}\right)$$

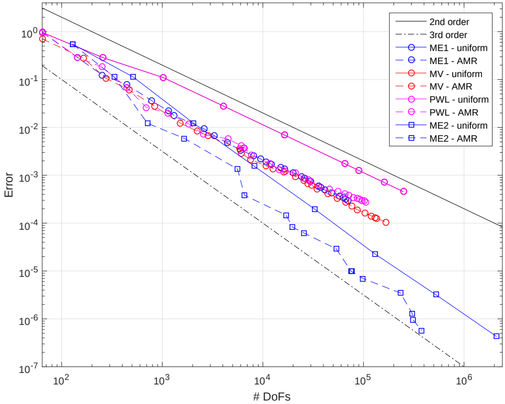

Linear ME cycle 15 (left) and quadratic ME cycle 08 (right)

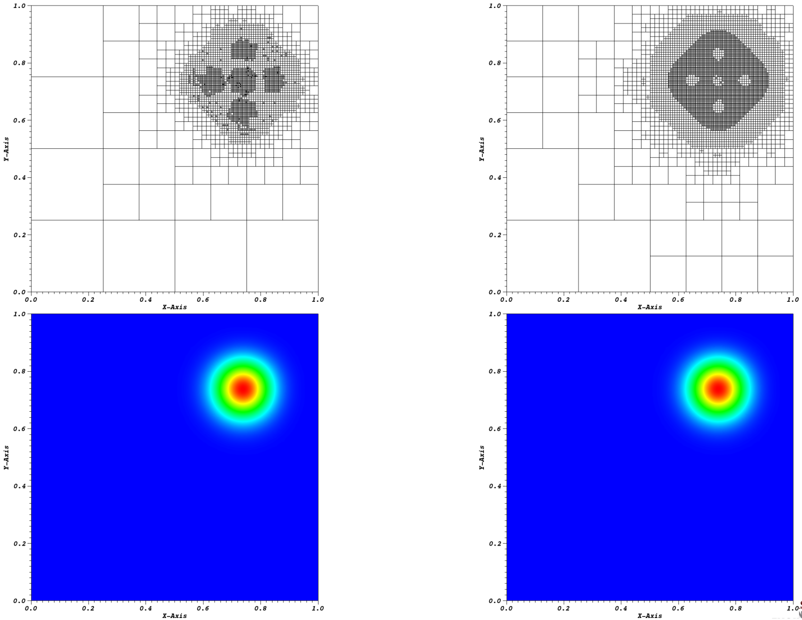

3D FEM/DSA Analysis

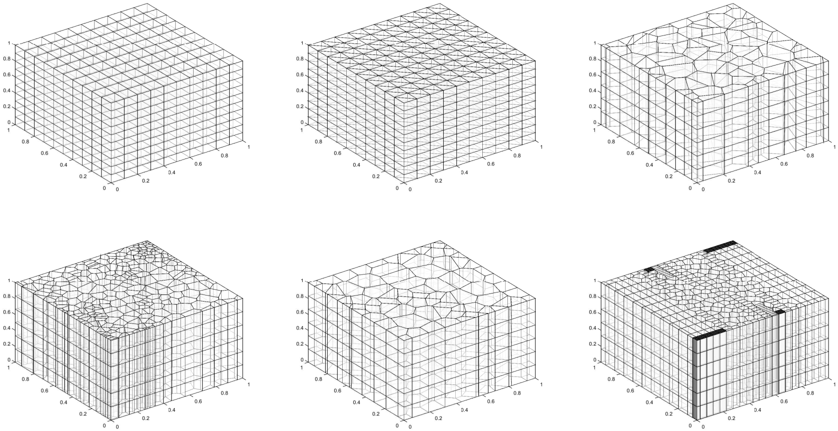

SIP exactly linear solutions on 3D polyhedral meshes using the PWL basis functions

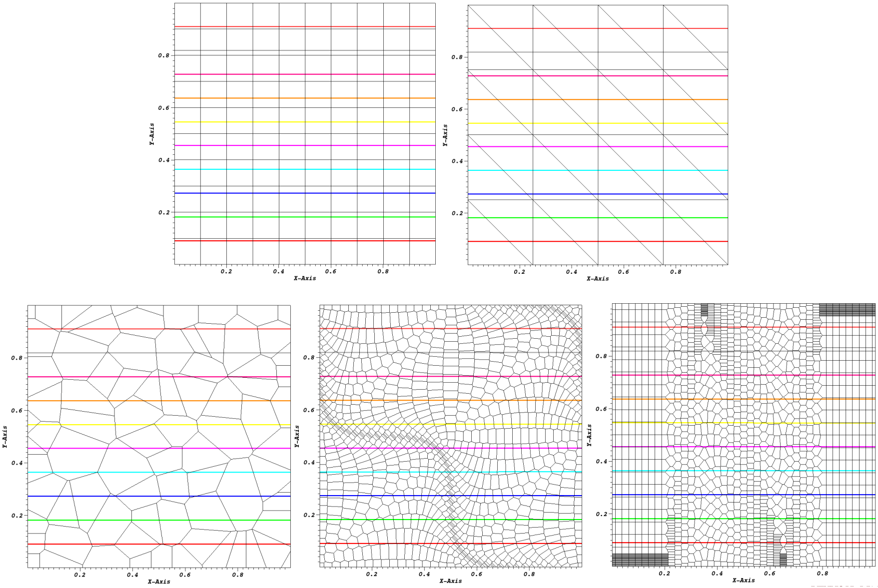

SIP convergence study - gaussian solution on 3D cube using the PWL basis functions

$$\Phi(x,y,z) = xyz(L_x - x)(L_y - y)(L_z - z)\exp(-(\mathbf{r}-\mathbf{r}_0)\cdot(\mathbf{r}-\mathbf{r}_0))$$
$$L_x = L_x = L_x = 1.0, \qquad \mathbf{r}_0 = (3/4, 3/4, 3/4)$$

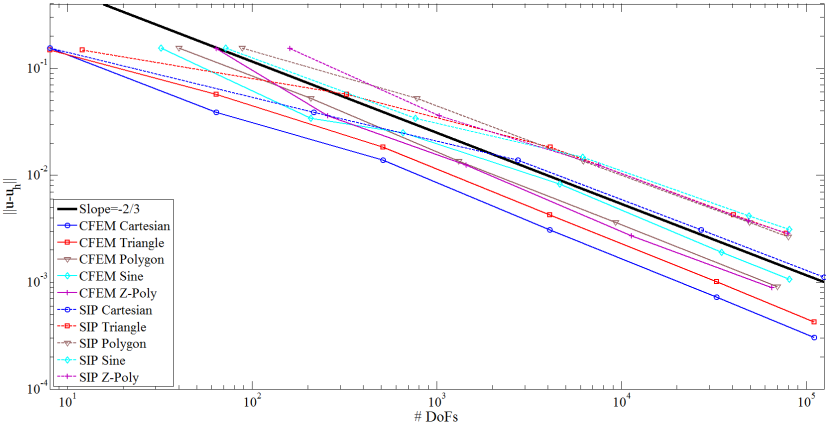

Fourier analysis - 3D PWL basis functions

$c = 1$

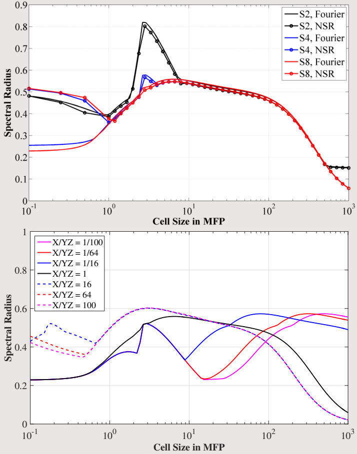

$c = 4$

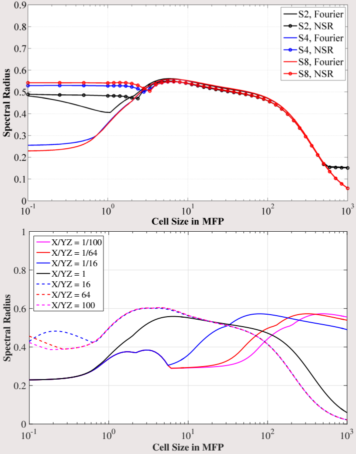

MIP DSA Timing Data with PDT on Vulcan using HYPRE

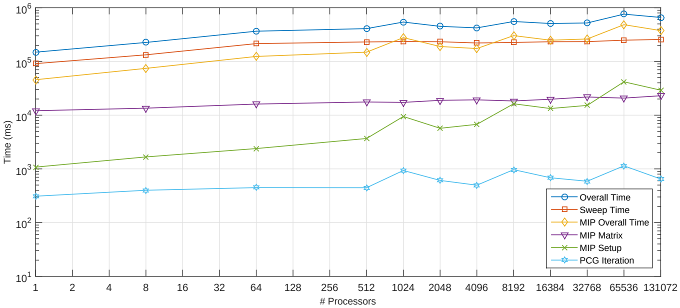

Problem Description

- Modified Zerr problem - used optimal sweep aggregation parameters
  - homogeneous cube - about 500 mfp and c=0.9999
  - $S8$ level-symmetric quadrature
- pointwise convergence tolerance of 1e-8
- SI precondition with MIP DSA using HYPRE PCG and AMG

Two-grid acceleration implementation in PDT

- Successfully implemented and debugged
  - Includes non-orthogonal mesh configurations
  - Includes multi-material configurations
- Have tested the two-grid methodology on a homogeneous graphite block as well as a block with an air duct
- Iteration counts for a very large configuration (very optically thick) are similar to simple infinite medium calculations

Materials	Unaccelerated Iterations	Accelerated Iterations
Graphite Only	2027	21
Graphite + Air Duct	2138	23

Work Summary and Status - completed (blue), in-progress (orange), and not-started (red)

POLYFEM

1. Analyze the 2D linear polygonal basis functions for use in DGFEM transport calculations
2. Perform the same analysis with the quadratic serendipity basis functions
3. Determine the effects of numerical integration on highly-distorted polygonal elements
4. Perform analysis on benchmark cases using polygonal meshes (including AMR)

MIP DSA

1. Analyze the 2D polygonal basis functions with MIP DSA preconditioning through Fourier/numerical analysis
2. Extend the analysis of MIP DSA to arbitrary convex 3D polyhedra
3. Analyze the effects of AMR with polygonal basis functions on the MIP DSA PCG iteration counts (with and without bootstrapping)
4. Implement MIP DSA in PDT using HYPRE
    1. Analyze the scalability of the method to high process counts
    2. Implement and perform analysis of two-grid acceleration
    3. Perform parametric studies on aggregation/partitioning factors - generate a performance model of MIP DSA with HYPRE
    4. Run realistic numerical experiments - IM1 and reactor geometries

I look forward to your feedback regarding my PhD Proposal

Questions?

A special acknowledgment to the Department of Energy Rickover Fellowship Program in Nuclear Engineering, which provides strong support to its fellows and their professional development.

Linear POLYFEM limits - Wachspress, mean value, and max entropy (Go back)

General form

$$\lambda_i(\mathbf{x}) = \frac{w_i(\mathbf{x})}{\sum_j w_j(\mathbf{x})}$$

Nodal limits - $\lim_{\mathbf{x}\to\mathbf{x}_j} \lambda_i(\mathbf{x})$

$$\lambda_i(\mathbf{x}) = \frac{w_i/w_j}{1+\sum_{k\neq j} w_k/w_j}, \qquad i \neq j$$

$$\lambda_j(\mathbf{x}) = \frac{1}{1+\sum_{k\neq j} w_k/w_j}$$

$$\lim_{\mathbf{x}\to\mathbf{x}_j} \frac{w_k(\mathbf{x})}{w_j(\mathbf{x})} = 0, \qquad k \neq j$$

$$\therefore \lambda_i(\mathbf{x}_j) = \delta_{ij}$$

Edge limits - $\lim_{\mathbf{x}\to\mathbf{x}^*} \lambda_i(\mathbf{x})$, $x^* \in e_j$

$$\lim_{\mathbf{x}\to\mathbf{x}^*} |w_i(\mathbf{x})| = \infty, \qquad i = (j, j+1)$$

$$\lim_{\mathbf{x}\to\mathbf{x}^*} |w_i(\mathbf{x})| < \infty, \qquad i \neq (j, j+1)$$

$$\lim_{\mathbf{x}\to\mathbf{x}^*} \lambda_i(\mathbf{x}) = \begin{cases} \frac{||\mathbf{x}_{j+1}-\mathbf{x}||}{||\mathbf{x}_{j+1}-\mathbf{x}_j||}, & i = j \\ \frac{||\mathbf{x}_j-\mathbf{x}||}{||\mathbf{x}_{j+1}-\mathbf{x}_j||}, & i = j+1 \end{cases}$$